DIAPHRAGM FORMING OF THERMOSET COMPOSITES

H.E.N. Bersee*, S. Lindstedt*, G. Niño*, Adriaan Beukers*,**
*** Delft University of Technology, Faculty of Aerospace Engineering**
PO Box 5058, 2600 GB Delft, The Netherlands
**** Fellow Professor Doshisha Uuniversity, Kyoto, Japan**

Keywords: *diaphragm forming, diaphragm wrinkling, interply fibre buckling, intraply fibre buckling, thermoset composites, diaphragm deformation.*

Abstract

Diaphragm forming is a thermoforming process which was originally developed for forming of thermoplastic composites. In this project a mini-autoclave (Pressclave [4]) has been used to deform Cycom® 977-3 thermoset prepreg into a hemispherical cavity. Experiments have been conducted on laminates with variations in thickness and varying temperatures during the forming phase. The effect of forming temperature and diaphragm types on inter- and intraply fibre buckling, deformation of fibre yarns, and diaphragm wrinkling has been investigated. [0/90]^{o} laminates with up to 16 layers have successfully been deformed without inter- and intraply fibre buckling, however, diaphragm buckling did occur. Diaphragm buckling increased with thinner and less stiff diaphragms. In order to optimize the process, a special tool, the Square Grid Analysis has been developed for measuring the deformations of the diaphragms.

1 Introduction

Hand lay-up combined with autoclave curing is a composite manufacturing technique which is still widely used in the aerospace industry. The main reasons are the confidence in this well established process and the high fibre volume fractions and low void contents which can be achieved due to the high pressures used in autoclaving. However, autoclaving mainly depends on the manual mould lay-up of prepreg material. Manual lay-up of high-curvature products is complicated and most of all a time consuming process. Consequently, the manufacturing costs are high and the process is unsuitable for large series. Many alternative processes are being developed among which automated tape laying, fibre placement and resin infusion are the most promising techniques.

Another process which may offer improved cost efficiency is diaphragm forming of thermoset prepregs. This technique offers the possibility of lay-up and consolidation of flat prepreg stacks onto a high-curvature mould in a single step. Furthermore, product quality improves as manual lay-up is avoided. In combination with automated tape lay-up, diaphragm forming of thermoset prepreg could offer a significant reduction in part cost compared to conventional techniques [1].

2 Diaphragm forming

Diaphragm forming is a thermoforming process which was originally developed for forming of thermoplastic composites. In this process a laminate is placed between two foils (diaphragms). These diaphragms are clamped onto a mould after which in between a vacuum is applied (Fig.1). This package is placed in an autoclave and heated to the process temperature. After reaching this temperature a hydrostatic pressure difference is created, which forces the laminate/diaphragms into the mould. Due to the use of an autoclave, i.e. forming by a hydrostatic pressure and isothermally heating by a hot gas, products of a reproducible, high quality can be realized with this process. The processing cycle is very long, namely 1-2 hours, especially compared with the other thermoforming processes for thermoplastic composites, like press forming. This restricts the process to the production of small series of large products, like e.g. the skin of the leading edge of the Airbus A380 which is currently made by hand lay-up. Most aerospace industries have autoclaves, the investment costs for diaphragm forming therefore, can be low while due to sizes of the used autoclaves, the products can be quite large.

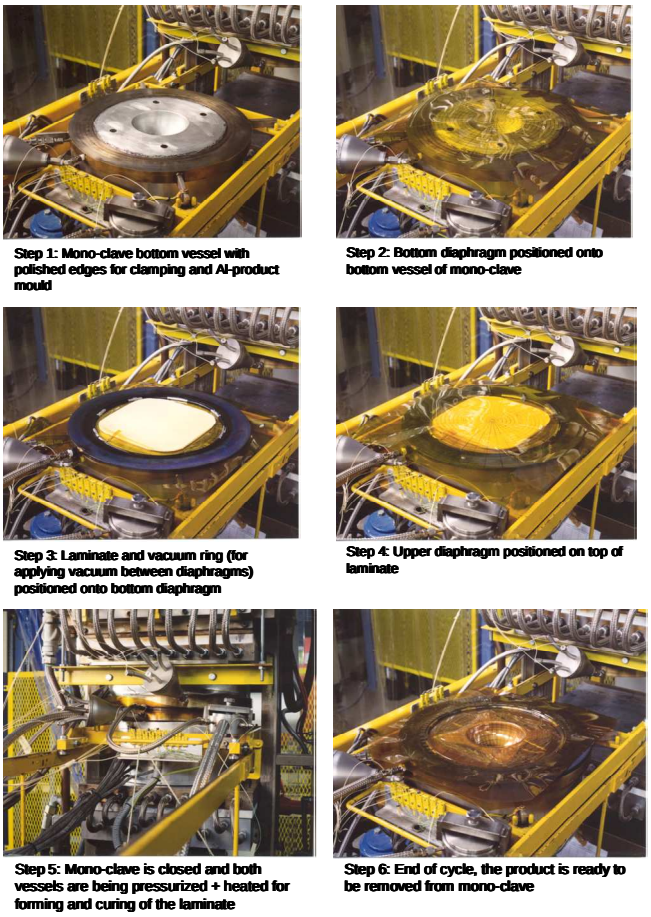

Fig. 1: Diaphragm Forming of Thermoplastic Composites

Consequently, diaphragm forming is very interesting for the aerospace industry, for the production of small series of large parts.

iaphragm forming of thermoset prepreg is similar to that of thermoplastic composites. However, the difference lies in the fact that the thermoset matrix is not melted prior to the forming phase but only heated to decrease the matrix viscosity sufficiently to enable the prepreg to be formed. Furthermore, instead of cooling the laminate immediately after the forming phase has finished, the temperature of the laminate is increased to the matrix's cure temperature after which the matrix undergoes a cure cycle. In essence, the diaphragm forming process for thermoset prepreg is an autoclave curing process in which a single-step forming phase has been incorporated. This single-step forming phase is the strong point of the process; it avoids the time consuming manual lay-up of prepreg onto the production mould prior to an autoclave process. Human input is reduced to preparation of the flat laminate-diaphragm package, and this could be taken over by automated tape lay-up. Another advantage of diaphragm forming over hand lay-up is that de-bulking is not necessary anymore, which especially for thick laminates can reduce the labour cost significantly.

Previous research has shown that it is possible to apply the diaphragm forming process to thermoset prepreg; MT6-D (Advanced Composites Group) prepreg had successfully been formed into 3D-elements [3]. This paper describes diaphragm forming-experiments that were conducted on Cycom® 977-3 prepreg (Cytec).

3 Experimental

3.1. Test set-up

Diaphragm forming of the Cycom® 977-3 prepreg was conducted in a mini-autoclave called Pressclave or Monoclave. This apparatus has been designed as a mobile unit, which can easily be placed in and out a flat platen press and consists of

an autoclave part, pressure valves, control units, a vacuum pomp, and the necessary plumbing. The autoclave part is formed by two hat shaped pressure vessels, which have polished edges for airtight clamping. The lower vessel contains a mould with a hemispherical mould cavity (100mm diameter) (Fig. 3a). The transition from the flat part of the mould into the cavity is slanted. The lower pressure vessel is mobile, while the upper vessel is fastened to the flat platen press. During the diaphragm forming process, the flat platen press presses the two vessels against each other so that an airtight autoclave is created.

Band heaters placed around the vessels supply heating. The platens of the press also provide heating, and these are used for cooling. Temperature is monitored by thermocouples located in the lower and upper pressure vessel, in the mould, and in the vacuum ring. Pressure is controlled by pressure sensors in the upper and lower pressure vessels. Nitrogen is used as pressure medium and is supplied from a gas bottle. The hydrostatic pressure difference necessary for the forming process is created by decreasing the pressure in the lower vessel.

After the prepreg/diaphragm stack is placed onto the mould, the bottom vessel is moved into the flat platen press, a vacuum is drawn between the diaphragms through the vacuum ring, and the upper and lower vessel are pressurised to the curing pressure (6bar). The sample is heated to the required forming temperature by heating the upper and lower vessels. At the forming temperature, the forming phase is initiated by decreasing pressure in the lower pressure chamber at a constant rate of 1 bar/min. This causes the diaphragms together with the prepreg stack to be pushed into the mould cavity. As soon as the forming phase reaches its end, the prepreg is heated to the curing temperature of 180ºC, followed by a one-hour cure at 6bar. Finally, the sample is cooled and removed from the mould.

The bottom vessel contains an aluminium mould with a hemispherical cavity (100 mm radius) on which the lower diaphragm is placed. Then a vacuum ring is positioned on the bottom vessel and thermocouples are located near the edge of the laminate. A ring of breather material is placed against the vacuum ring to create a proper vacuum between the diaphragms and thereby ensures a proper fixation of the prepreg above the mould cavity. Next step is the positioning of the laminate and placement of strands of carbon fibre running from the breather ring to the edges of the laminate. These carbon fibre strands are used for venting air out of the laminate. The final step in the preparation is the positioning of the upper diaphragm after which the whole build-up is moved into the flat platen press.

3.2 Materials

The following materials were used for the experiments:

- Test samples: CYCOM® 977-3 prepreg, with carbon fibre crowfoot satin weave (Cytec); 210x210mm with rounded corners (40mm radius).
- Diaphragms:
  - 75µm Capran 988 Nylon film (Aerovac Systems); 470x470mm.
  - 100µm Capran 980 Nylon film (Aerovac Systems); 470x470mm.
  - 100µm Elastomax 1000 Nylon film (Aerovac Systems); 470x470mm.
- Release agents: Frekote 44-NC; four layers were applied on the prepreg side of both diaphragms; one layer was also applied on the mould prior to each experiment.
- Breather material: Thick glass fibre braid and carbon fibre roving.
- Laminates: $0/90^{o}$ lay-up and 2, 8 and 16 prepreg layers.

4 Results

The purpose of this study was to investigate the potential of diaphragm forming for manufacturing of thermoset composites. Therefore, the first criterion for evaluation of the tests was the conformity of the part to the mould. Therefore, all samples were visually inspected for complete deformation. In addition, the diaphragms were visually inspected on ruptures. Furthermore, thickness measurements were performed on sixteen-layer samples to determine the effect of the diaphragm forming process on local part thickness. From the diaphragm forming tests, the following defects and phenomena were observed in the products and diaphragms:

1. Lines of resin on the upper surface of the hemisphere due to wrinkling of the upper diaphragms.
2. Interply fibre buckling due to a combination of in-plane compression stresses and poor lubrication between fibre layers. As a result, fibres tend to buckle out of plane.
3. Intraply fibre buckling due to exceedance of the maximum shearing angle of a fabric during the deformation process. This type of fibre buckling leads to wrinkles in the fabric.
4. Transverse flow of the fibres (or fibre slipping) due to an applied pressure; the fibres get “squeezed” transverse to the fibre direction.

These phenomena were used in the evaluation of the tests. A distinction was made between “upper” and “bottom” surfaces and diaphragms, where the bottom surface and bottom diaphragm are facing the mould cavity.

The first experiments were conducted on two-layered prepreg stacks at temperatures of 50, 70, 90, and 110ºC and a forming pressure of 6bar with a forming rate of 1bar/min. The samples were formed with 75µm thick Aerovac Capran 988 diaphragms.

The 6 bar forming pressure was sufficient for forming all samples in the temperature range of 50 to 110ºC. No signs of interply and intraply fibre buckling were seen on the samples (Fig. 4). However, the upper surfaces of all samples showed

lines of resin due to diaphragm wrinkling, mainly on the slanted part (Fig. 5). The number and size of these resin lines increased with increasing forming temperatures from 50 to 90ºC. Increasing temperatures reduces the diaphragms critical buckling stress; the wrinkles in the diaphragms are filled with resin, which afterwards shows as resin lines on the surface. However, at 110ºC the resin lines decreased both in size and in number, as the resin flowed out of the diaphragm wrinkles because of the low resin viscosity at 110ºC.

Upper surface

Lower surface

Fig. 4: Diaphragm formed two-layered sample

On the bottom surface of the samples, pin holes were found (Fig. 6). These pin holes had formed along lines between adjacent fibres and at locations were fibres interlace. The amount and size of these pin holes decreased with increasing temperatures, and were no longer present at 110ºC. At lower temperatures, the resin viscosity might be too high for adequate resin flow into the gaps between fibres.

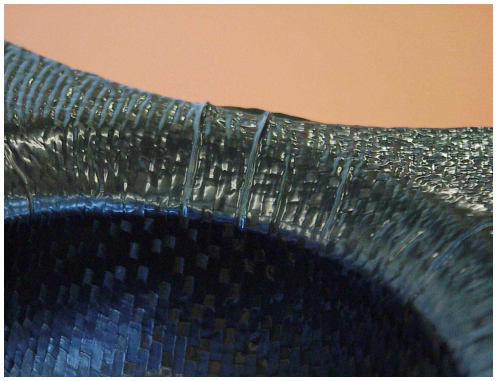

Fig. 5: The effect of diaphragm wrinkling

Fig. 6: Pjn holes on bottom surface

Fibre slipping was another phenomenon that occurred (fig. 7). Fibres in the corners of the laminate (around the diagonals of the blank) have to shear in order to conform to the deformation of the fabric into the mould. As a result, the fibre angles shift. However, the fibres between the corners must slip transverse to their longitudinal axis in order to conform to deformation. As a result, transverse fibre slipping had occurred in all samples on the bottom surface, especially where the slanted area changes into the hemispherical part. At this location, the bottom surface fibres are clamped onto the mould almost immediately at the start of the forming process. As a result, fibres in the hemispherical part have to slip considerably in order to conform to the mould. The fibres on the upper surface however, showed less fibre slippage, as the outer fibre plies can move relative to the inner plies and do not become clamped due to the lubricating effect of the resin. Therefore, fibre slippage can be spread over a larger part of the fibres. The amount of fibre slip did not noticeably change with increasing temperature.

As diaphragm forming of 2-layer samples posed no major problems, the amount of layers was increased to eight. This sample was formed with 75µm thick Capran 988 diaphragms at a temperature of 110ºC and 6 bar forming pressure (forming rate 1

bar/min). The result was a completely formed sample without any rupture of the diaphragms. However, the lower diaphragm had become so thin on the pole of the part that it was impossible to remove it without tearing. The extreme thin spot in the bottom diaphragm can be explained by the fact that the diaphragm is clamped onto the equator of the mould cavity as soon as forming starts. Hence, all diaphragm deformation had to come from the area above the mould cavity. The upper diaphragm was not clamped and could therefore deform much more uniformly over its area so extreme thin spots were not created. The upper diaphragm could easily be released in one piece.

Compared to the deformations and defects in the 2-layer samples there were some differences. The eight-layer samples showed local increase in thickness along the flat and slanted areas. Furthermore, no bottom diaphragm wrinkling had occurred. However, on the upper surface the size of the diaphragm wrinkles had increased compared to those on the two-layer samples. The larger resin lines due to diaphragm wrinkling (Fig. 8) might be explained by the thickness increase on the slanted and flat area of the sample. The thickness of the laminate locally increases due to shearing of the fibres, and such a thickness increase can push the diaphragm in the out of plane direction. In combination with compressive stresses in circumferential direction, this further facilitates diaphragm buckling.

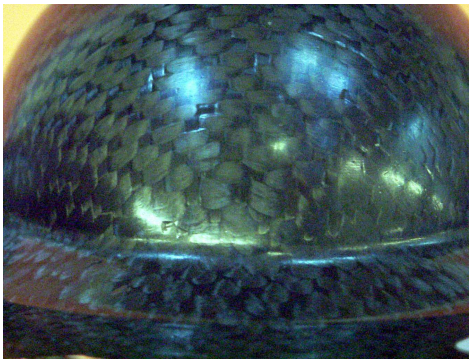

Fig 7: Fibre slip

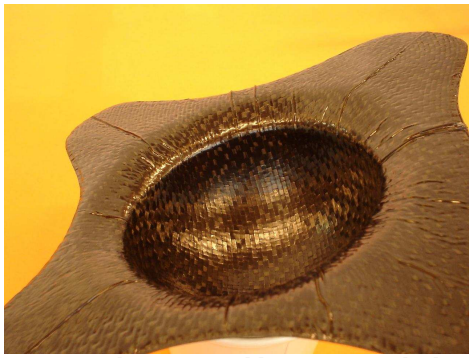

Fig. 8: Diaphragm wrinkling in an eight-layer sample

The extreme thinning of the bottom diaphragm might cause premature rupture during the forming of even thicker samples, which happened for the first sixteen-layer sample (forming at 110ºC and 6bar (1 bar/min)); the bottom diaphragm had ruptured (Fig.

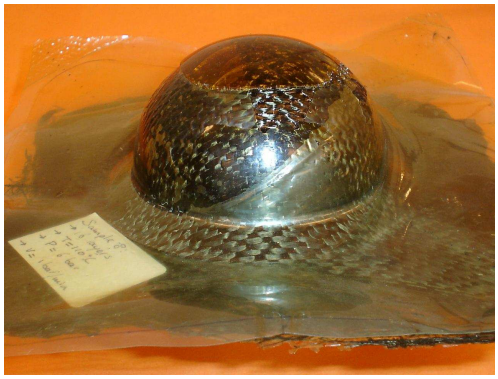

bottom surface

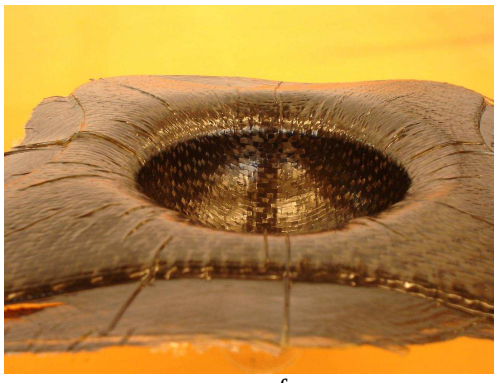

upper surface

Fig. 9: Sixteen-layer sample formed with 75µm diaphragms

bottom surface

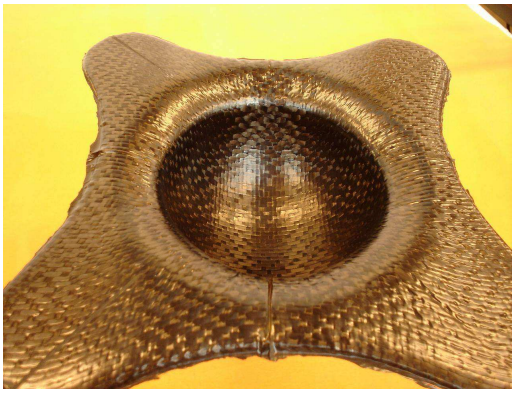

upper surface

Fig. 10: Sixteen-layer sample formed with 100µm diaphragms

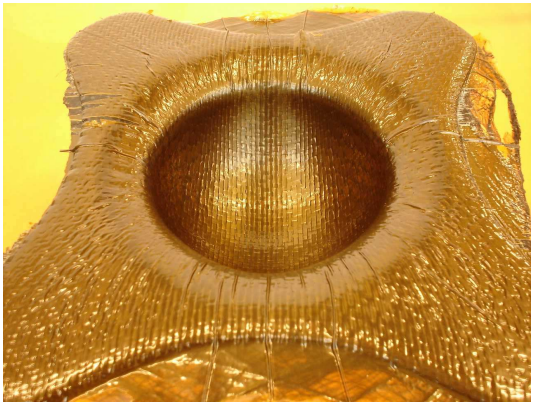

Fig. 11: Sixteen-layer sample formed with Elastomax 1000 diaphragms

9). This first sixteen-layer sample showed more upper diaphragm wrinkling than the eight-layer samples, which is caused by the large thickness increase of the laminate in these areas.

In order to prevent diaphragm rupture, thicker (100 μm) diaphragms were used. As can be seen in Fig.10, the laminates were deformed completely. The appliance of a thicker diaphragm also resulted in a decrease of diaphragm wrinkling due to the higher diaphragm stiffness. To investigate the influence of the diaphragm stiffness, a test was perfomed with a 100μm thick Elastomax 1000 nylon film, which has a lower E-modulus than the Capran 980 film. The laminate was completely deformed (Fig. 11), but it was impossible to release both upper and bottom diaphragms from the finished part, even though the Elastomax diaphragms had been treated with the same release agent as the Capran diaphragms. The sample also showed more and larger wrinkles compared to Capran 980 sample, which is an indication, that diaphragm wrinkling increases with reducing diaphragm stiffness.

5. Diaphragm deformation

As was mentioned in the previous paragraph, the upper and bottom diaphragm show a different deformation mechanism. In a previous study [2] on diaphragm forming of thermoplastic composites (glass fabric reinforced PEI of Ten Cate Advanced Composites), the deformation of the diaphragms was determined. The diaphragms were provided with a grid for determination of the extension ratios. This grid consisted of circles and radial lines, which were made by silk-screen printing. The ink lies on top of the diaphragm and was dried at 120 ^{o}C. In this way the diaphragms were not affected by the printing. The ink turned out to be resistant to high temperatures and although it lies on the surface of the diaphragm, it did not vanish during forming.

The extension ratios were calculated from the deformations of the grid. The diaphragm is an initially flat sheet which is forced into the shape of an axisymmetric shell of revolution. This results in a deformation of a segment as illustrated in Fig.12. A segment is an originally annular ring (with inner radius r_0, width δr_0 and thickness h_0), which moved to the position as indicated in the figure, with r, δl and h as the new inner radius, width and thickness, respectively. The extension ratios may be written as [ref.5]:

$$\lambda_1 = \frac{\delta l}{\delta r_0}$$
$$\lambda_2 = \frac{r}{r_0} \qquad (1)$$
$$\lambda_3 = \frac{h}{h_0}$$

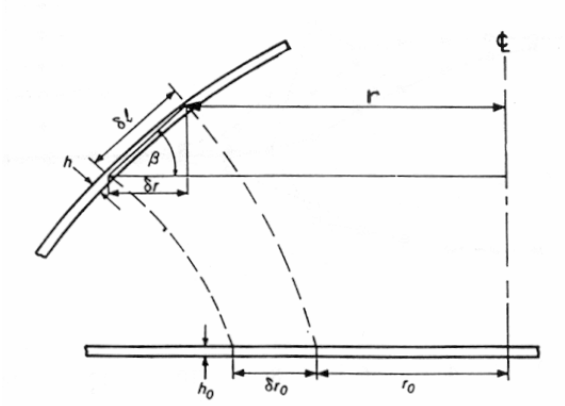

Fig.12: Deformation of a segment of the diaphragm

The width δl of the deformed segment is measured by a flexible ruler. In order to prevent deformation of the diaphragm during measurement, it is positioned on top of a glass/PEI hemisphere produced in the preliminary tests. The thickness is measured by using a LVDT, in order to prevent the influence of the curvature of the segments on the thickness measurement the diaphragms were cut into pieces. The average initial thickness h_0 is 0.1278 mm with a tolerance of ± 0.004 mm. Extension ratio λ_2 is calculated with point 0 being the pole of the hemisphere, taken as a reference since this is the only point on the grid that does not move during a test. The length r can not directly be measured and is, therefore, calculated by the following expression:

$$r = R * \sin\left(\left(\sum_{i=0}^{i=n} \delta l_i\right) / R\right) \qquad (2)$$

points at spherical part

$$r = R + \left(\left(\sum_{i=0}^{i=n} \delta l_i\right) - R * \frac{\pi}{2}\right) + \sum_{i=n}^{i=15} \delta l_i \qquad (3)$$

points in flat area, where;
R= radius of hemisphere (70 mm)
δl_i= width of segment I

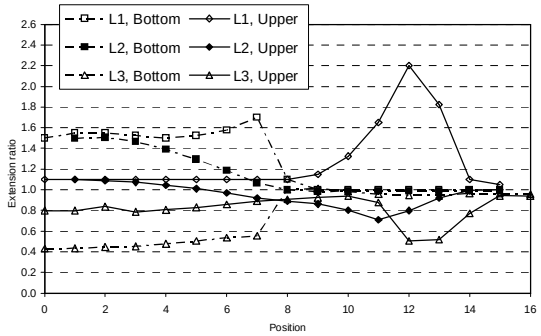

Fig. 13: Deformation of bottom and upper diaphragm in forming of thermoplastic composites

The validity of the measurements is checked by calculating the deviation of the extension ratios with the constant volume assumption:

$$\lambda_1 \lambda_2 \lambda_3 = 1 \qquad (4)$$

In Fig.13, a representative graph is shown of the deformation of the diaphragms. As can be seen, the bottom diaphragm only shows a deformation in the area above the mould cavity (position 0-8), outside the mould cavity there is no deformation. This means that prior to forming the bottom diaphragm is clamped onto the mould. The upper diaphragm on the contrary shows only a small more or less uniform deformation in the area above the mould cavity and a large deformation outside the mould cavity. This is the area of the large sliding of the laminate due to the intraply shear of the fabric (area X in Fig.10). It can thus be concluded that only the upper diaphragm can prevent fibre wrinkling by acting as a blank holder.

6. Square grid analysis tool

The study showed that diaphragm forming can be used for the manufacturing of thermoset components. However, the process needs to be optimized since diaphragm and fibre wrinkling occurs, which is considered to be unwanted. To optimize the process an in-depth study into the behaviour of the diaphragms is necessary. Before this study can be performed a tool has to be developed which can measure the deformation of the segments of the diaphragm, since in the previous study this was done manually.

The square grid analysis technique is a well-known experimental method used for strain analysis in metal forming processes [6, 7], and it has been adapted to investigate thermoformed composites [8,9]. The technique uses a known array placed or attached to the sample surface prior to deformation. This pattern is distorted as it deforms with the surface, but it stays visible in spite of high forces involved during forming [10]. Thus, the resulting deformation pattern can be measured utilizing calibrated transparencies, transducers, digitizers or optical methods [9]. The information gathered can be used to assess composite fabric deformations, foil strain behavior and to validate manufacturing simulation tools.

A classical approach to study the deformation of diaphragm foils has used spider web shape grids. However, in order to automatize the measurement and analysis process, a rectangular grid has proved to be more efficient as it is depicted in Figure 14. The grid has been printed using special inks suitable for high temperature, friction and foil deformation conditions. The ink has to warranty the grid geometrical stability and adherence to the foil.

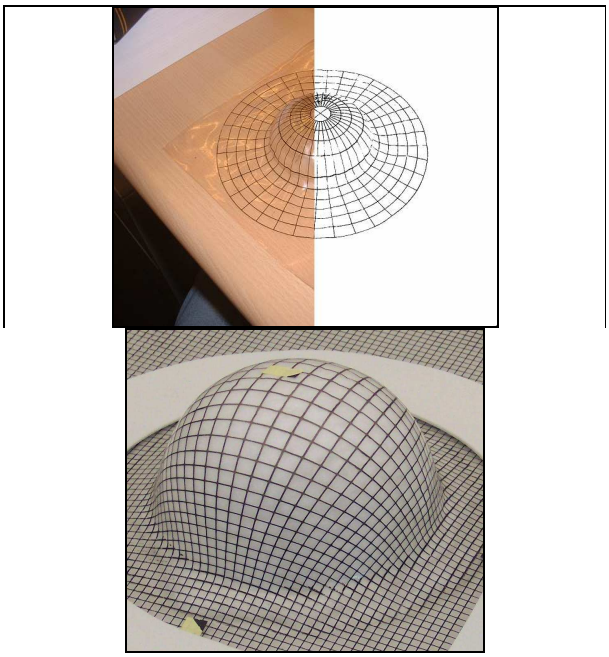

Fig. 14. Spider web grid (left) and square grid (right) for strain analysis on diaphragm foils.

After the deformation of the diaphragm, the foil is placed on a set-up as shown in Figure 15, where a target is placed near to the specimen. A region of interest, based on the geometry of the specimen, is selected for analysis. Then, the user takes a series of pictures of the product from different perspective views with a video or digital camera. From the photos, the deformed array

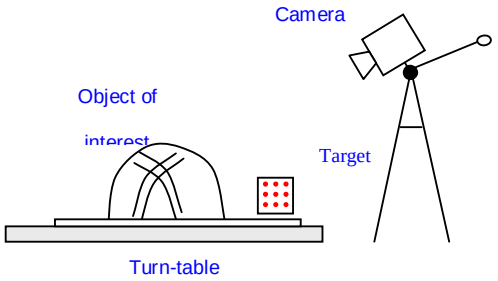

Fig. 15. Square Grid Analysis set-up

position is localized and with two or more images, the global 3D or global coordinates are computed using perspective projection geometry. The relationship between the global coordinate system and the image coordinate system is performed by camera calibration using the known target geometry. Finally, the obtained global coordinates are used to compute the strains for each deformed square on the foil.

It is well known that a way to describe the geometric aspect of an object that forms one image is using projective geometry and its perspective projections. The perspective is the projection of a 3D object onto a 2D surface by straight lines that pass through a single point. This point is called the projection or camera center C and it can be the origin of a 3D coordinate system whose Z-axis is along the optical axis [See Figure 16]. Now, if a point P on an object with global coordinates (X,Y,Z) is registered as p on some image plane at a focal length f from C, it will have the image coordinate (x,y). The relationship between the two coordinate systems is given by:

$$x = \frac{Xf}{Z} \quad and \quad y = \frac{Yf}{Z} \tag{5}$$

The use of homogeneous coordinates [6] can linearize the Eqn. 5 in function of the pixel coordinate system as follows

$$\begin{bmatrix} su \\ sv \\ s \end{bmatrix} = \begin{bmatrix} \frac{f}{pixel\ \ width} & 0 & u_c & 0 \\ 0 & \frac{f}{pixel\ \ heigth} & v_c & 0 \\ 0 & 0 & 1 & 0 \end{bmatrix} \begin{bmatrix} X \\ Y \\ Z \\ 1 \end{bmatrix} \tag{6}$$

Where, s is a scale factor. The Eq.6 can be rewritten in matrix notation as

$$\tilde{\mathbf{u}} = \mathbf{P} \cdot \mathbf{M} \tag{7}$$

where:

$\tilde{\mathbf{u}}$ = Image pixel coordinate homogeneous vector

$\mathbf{P}$ = Perspective projection matrix

$\mathbf{M}$ = Global coordinate homogeneous vector

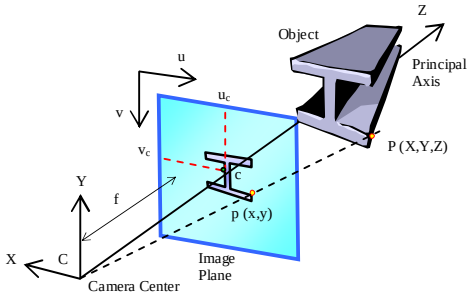

Fig.16. Camera and global coordinate systems

In general, the 3D global coordinate system may not be aligned with the camera. Therefore, a modification in the Eqn. 7 must be included to take in account this case as follow

$$\tilde{\mathbf{u}} = \mathbf{P} \cdot \mathbf{K} \cdot \mathbf{M} \tag{8}$$

where, **K** is a camera transformation matrix. Finally, the matrixes **P** and **K** can be rewritten into a single matrix **C** called the *Camera Calibration Matrix*.

The relationship between the global coordinates and the pixel coordinates is obtained by camera calibration using the known target placed on each picture. On this paper, a steel cube of 40mm with an array of nine holes per face was used as target, and it defines the global coordinate whose origin is in one of its base corners. Thus, the calibration matrix C is obtained solving the Eqn. 9.

$$\mathbf{B} \quad \mathbf{C} = \mathbf{UV} \tag{9}$$

Where, **B** is a matrix of constraint coefficients; **C** is the unknown calibration matrix, and **UV** is an image coordinate vector of the target points. Once the matrix **C** is known for each image, then any image point P with unknown X, Y, and Z coordinates, that projects onto the two image planes at (u,v) and (u',v'), will satisfy the Eqn.9.

$$\begin{bmatrix} C_{11}-uC_{31} & C_{12}-uC_{32} & C_{13}-uC_{33} \\ C_{21}-vC_{31} & C_{22}-vC_{32} & C_{23}-vC_{33} \\ C'_{11}-u'C'_{31} & C'_{12}-u'C'_{32} & C'_{13}-u'C'_{33} \\ C'_{21}-v'C'_{31} & C'_{22}-v'C'_{32} & C'_{23}-v'C'_{33} \end{bmatrix} \begin{bmatrix} X \\ Y \\ Z \end{bmatrix} = \begin{bmatrix} uC_{34}-C_{14} \\ vC_{34}-C_{24} \\ u'C'_{34}-C'_{14} \\ v'C'_{34}-C'_{24} \end{bmatrix} \quad (10)$$

Then, solving Eqn. 10, the global coordinates of the studied region or surface are found. Once the global coordinates are known, they are used to perform a 3D reconstruction of the region of interest and to compute engineering or true strains for each deformed square. This surface is created using patches and its smoothness depends on the number of grid points selected. However, a better surface can be obtained using these points as reference coordinates for high-order surfaces or using surface fitting methods [12]. As application case, the ε_x and ε_y strains for a diaphragm formed polyamide Capran980, as the one shown in Figure 14, are depicted in Figure 17.

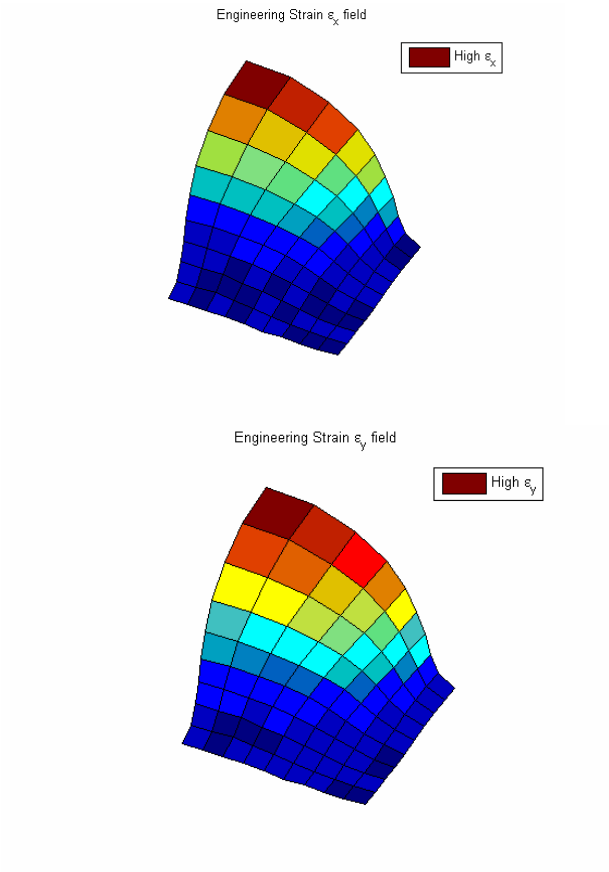

Fig.17 .Engineering strains for x(left) and y (right) direction for a Capran980 diaphragm.

7 Conclusions

Diaphragm forming is a thermoforming process initially being developed for thermoplastic composites. Experiments with diaphragm forming of Cycom 977-3 prepreg have shown that this manufacturing process can also be applied to thermoset composites. The great advantage is that the process offers the possibility of forming a flat prepreg stack into highly curved parts with a high quality. The time-consuming manual lay-up of prepreg on contoured moulds can be avoided, which is particularly advantageous in the case of thick components. Diaphragm forming can be applied to prepreg stacks as thick as sixteen layers.

However, forming thick laminates does require the use of thick and stiff diaphragms; 75µm diaphragms can get too thin during the forming process, which can lead to diaphragm rupture and to problems with releasing diaphragms from finished parts. Furthermore, thicker and stiffer diaphragms prevent excessive diaphragm wrinkling. However, to further optimize the process, an in-depth study into the behaviour of the diaphragms is required. Previous research has shown that the deformation of the upper diaphragm is different from the bottom diaphragm. The bottom diaphragm only shows deformation in the area above the cavity, while the upper diaphragm only in the area of fibre shearing.

In a previous research project, the deformations of the diaphragms were measured by hand. The results were reasonably accurate with an error of 10%. However, to investigate the differences in deformation of diaphragms with varying E-modulus and thickness, a more accurate and contact less tool has to be developed. In this project a Square Grid Analysis Tool has been developed. The first trials showed that the diaphragm deformations could be measured

Acknowledgements

The authors would like to thank Aerovac Systems Limited for supplying the nylon diaphragm material and Stork Aerostructures for supplying the Cytec 977-3 prepregs..

References

[1] Gutowski T.G., Dillon G., Chey S. and Li. H, "Laminate wrinkling scaling laws for ideal composites", *Composites Manufacturing 6*, Elsevier Science Limited, Great Britain, 1995, pp. 123-134.

[2] Bersee H.E.N., *"Diaphragm Forming of Continuous Fibre Reinforced Thermoplastics"*, Phd Thesis at Delft University of Technology, Delft University Press, the Netherlands, 1996.

[3] Wittenhorst K. van, *"Diaphragm Forming of Continuous Fibre Reinforced Plastics"*, Thesis at Delft University of Technology, the Netherlands, 1996.

[4] Lindstedt S., Bersee H.E.N., "Diaphragm forming of thermoset composites – Feasibility study of diaphragm forming of Cycom® 977-3 prepreg", *Tech report at Delft University of Technology*, the Netherlands, 2003.

[5] Williams J.G., *'Stress analysis of polymers'*, second edition, Chicester

[6] Sklad M.P., "Aspects of automated measurement of proportional and non-proportional deformation in sheet metal forming." *Materials Processing Technology*, Vol .145, p. 377-384, 2004.

[7] Manthey D.W. and Lee D., "Vision-based surface strain measurement system". *Journal of Materials*, Vol.47(1), p. 46-49, 1995.

[8] Nino, G.F., Bergsma O.K., and Bersee H.E.N. "Square grid analysis for intraply shear in thermoformed thermoplastic composites. in Second International Conference on Composites", *Testing and Model Identification COMPTEST*, Bristol, UK, 2004

[9] Nino G.F., Bergsma O.K., and Bersee H.E.N., "Evaluation of intraply shear in thermoformed composite products. in 15th International", *Conference on Composite Materials ICCM*, Durban, South Africa, 2005.

[10] Galanulis, K., "Optical measuring technologies in sheet metal processing", *in www.gom.com, GOM Gesellshaft fur Optische Messtechnik mbH.*

[11] Faugeras, O. and Luong Q.T., *"The geometry of multiple images"* Cambridge, MA. USA: The MIT Press, 2001.

[12] Christie, G.R., *"Numerical modeling of fiber-reinforced thermoplastic sheet forming"*, in Department of Mechanical Engineering. 1997, University of Auckland, New Zealand: Auckland.